Numerical investigation of the dynamics of pressure loading on a solid boundary from a collapsing cavitation bubble

[1]Prasanta Sarkar*; [1]Giovanni Ghigliotti; [2]Marc Fivel; [1]Jean-Pierre Franc

*[1]Univ. Grenoble Alpes, CNRS, Grenoble INP**, LEGI, 38000 Grenoble, France; [2]Univ. Grenoble Alpes, CNRS, Grenoble INP**, SIMaP, 38000 Grenoble, France*

Abstract

The motivation behind this research lies in understanding the physical mechanism of cavitation erosion in compressible liquid flows, with applications in the field of aerospace, hydrodynamics, diesel injectors etc. As a consequence of collapsing vapor cavities in cavitating flow near solid boundaries, high pressure impact loads are generated. These pressure loads are believed to be responsible for the erosive damages on solid surface observed in most applications. For our investigation, the initial geometry is a single vapor bubble near a solid boundary collapsing due to the pressure difference between the bubble and surrounding liquid. The numerical approach employs a simplified homogenous mixture or '*single fluid*' model with barotropic assumption in a fully compressible finite-volume fluid solver. The numerical method is validated against the well-known Rayleigh collapse of a pure *3D* vapour bubble. It is then used for the simulation of a *2D* vapour bubble collapsing in the proximity of a solid boundary placed at a specified distance from the centre of the bubble. The pressure loads are computed from the evolving dynamics of collapsing bubble near a solid boundary which can be used to determine the resulting surface deformation. The developed compressible cavitation solver in the *CFD* code *YALES*2 can efficiently model small and large scale cavitating structures in a fully resolved three dimensional flow.

Keywords: cavitation; cavitation erosion; bubble dynamics; fluid-structure interaction

Introduction

The collapse of cavitation structures formed due to the breaking down of the continuous liquid medium under very low pressures, near a solid surface leads to surface damage known as cavitation erosion. The driving mechanism for the cavitating structures is the local decrease in liquid pressure below typically vapor pressure at a given temperature [1]. The cavitating regions consist number of cavitation bubbles due to the rapid growth of initially present air nuclei in the liquid flow. These cavitation bubbles move along the liquid flow until they collapse in the areas of high pressure and disappear. The presence of air nuclei, amount of dissolved gas in the flow are determining factors for the amount and size of cavitation bubbles. The motivation of this research is to numerically investigate the unsteady compressible cavitation bubble behaviour in a continuum liquid flow, with associated compressibility effects inside the flow domain. It will be used to predict accurately the material surface response to these small time-scale, highly unsteady flow characteristics. The vapor bubble collapse is usually characterized by the shrinking of bubble surface, acceleration of liquid flow towards the centre of bubble and shock propagation during the collapse. During the final stages of the collapse, due to the collision of bubble surface and liquid jet at the center, a high impulse shock wave is produced and propagated into the surrounding liquid. The collapse of a cavitation bubble close to a solid boundary is significantly affected by the non-dimensional *stand-off parameter* (γ), defined as the ratio of distance of the bubble center from the solid boundary to the maximum bubble radius. The dynamics of the bubble collapse and its interaction with the solid boundary such as the liquid micro-jet formation, splashing and surface erosion is strongly dependent on the stand-off parameter. Comprehensive description of the effect of the stand-off parameter may be found in the paper of *Philipp* and *Lauterborn* [2]. For an isolated bubble, the collapse is basically symmetric and a shock wave forms near the center of the bubble which propagates into the surrounding liquid. For an asymmetric bubble collapse near a solid boundary, a liquid re-entrant micro-jet pierces through the bubble surface opposite to the solid boundary accelerating one side of the bubble towards the opposite surface. The liquid jet is directed towards the solid boundary and the estimated speed of the micro-jet is usually very high, several hundred meters per second. Multiple shock waves are emitted due to the impact of the liquid jet with the opposite bubble surface and eventually, the solid boundary. The high amplitude, localized pressure impulse at the solid boundary due to the emitted shock and micro-jet results in material surface damage or erosion. The collapse of a pure vapor bubble surrounded by a liquid can be represented as

*Corresponding Author, Prasanta Sarkar: prasanta.sarkar@univ-grenoble-alpes.fr
**Institute of Engineering Univ. Grenoble Alpes

as figure 1 where P_{bubble} is the pressure inside the bubble and P_{liquid} is the surrounding liquid pressure such that $P_{liquid} \gg P_{bubble}$.

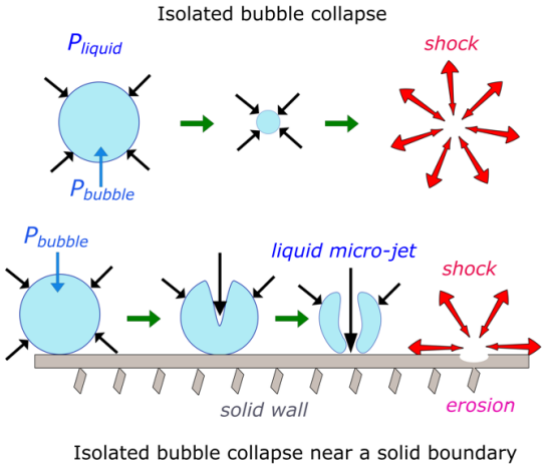

Figure 1: Vapor bubble collapse due to imposed pressure difference P_{liquid} >> P_{bubble}; collapse of an isolated bubble - symmetric collapse (top); bubble collapse near a solid boundary - asymmetric collapse (bottom)

Since one of the primary consequence of cavitation is its effect on nearby solid boundaries, a detailed investigation is needed on the final stage of bubble collapse with high temporal and spatial resolution. A feedback of solid material response can then be introduced into the fluid domain using a two-way coupled fluid-structure interaction model. The numerical investigation of collapsing cavitation bubble is challenging due to the need of high spatial and temporal resolution to capture the instantaneous high amplitude pressure loads.

CFD Solver *YALES2*

A pressure-based semi-implicit algorithm is used in the multi-physics solver YALES2 [3] for compressible flows with a fractional-step method [4] which is based on a characteristic splitting of the Navier-Stokes equation. The method consists of an advection or predictor step and a pressure-correction step separating the acoustics from the advection. In the pressure-correction step, a Helmholtz equation for pressure is solved implicitly to remove the acoustic *CFL* limitation. The compressible formulation of the governing flow equations allows its hyperbolic treatment to include the time dependent flow characteristics in the solution. Liquid flows with cavitation undergo strong negative pressure gradients for liquid break up to initiate cavitation. The speed of sound may be quite small in the two-phase region of a cavitating flow. For cavitation phase transition in a compressible liquid flow numerical methodology should resolve a wide range of Mach numbers (M), defined as the ratio of flow velocity to sound speed in the flow field. In the two-phase liquid-vapor mixture, local Mach number can be extremely high $M \gg 1$ whereas pure liquid phase stays close to low Mach number regime $M \to 0$. In the low Mach limit, the compressible $YALES2$ solver tends towards an incompressible solver inheriting the same stability and efficiency. In the solver, the wall boundary condition is treated implicitly by imposing a no-slip velocity in the advection or predictor step. Outlet boundary conditions are treated explicitly with classical Navier–Stokes Characteristic Boundary Conditions $(NSCBC)$ [5] to enforce acoustically non-reflecting boundaries. A consistent equation of state is used for the pure liquid phase using the Tait's equation of state and for the two phase liquid-vapor mixture following an isentropic phase transition model proposed in *Egerer et al.* [6]. The two phase modelling using a homogenous mixture or '*single fluid*' is widely accepted and implemented with the barotropic fluid assumption which specifies that the pressure is only a function of the fluid density. The model uses a single set of governing equations for all phases with consistent equations of state and fluid viscosities. Since the cavitation model is assumed to be barotropic, the energy equation is decoupled from the system of governing equations in the solver. The speed of sound in the pure liquid phase is computed as $c = \sqrt{\partial P/\partial \rho}$ whereas in the liquid-vapor phase it is constant equal to the speed of sound at ρ_L^{sat}. This is implemented to eliminate numerical instability of the pressure correction equation due to steep change in the speed of sound at the interface of pure liquid and liquid vapor mixture phase.

Results

The two phase model for compressible liquid is validated for an isolated *3D* single bubble collapse case with the analytical model of Rayleigh-Plesset described in [1]. The analytical model considered assumes liquid incompressibility and no liquid viscosity, gravity and surface tension. The analytical model considers a bubble saturated with pure vapor whose pressure is equal to vapor pressure $P_{vap} = 2194\ Pa$ at $292.15\ K$ and surrounding liquid pressure $P_{\infty} = 10\ MPa$. The numerical simulation is carried out with a bubble initially filled with two phase mixture of 99% saturated vapor content inside or simply, a vapor void fraction $\alpha = 0.99$ corresponding to a pressure of $2194\ Pa$ at temperature $292.15\ K$ and liquid-vapor mixture density of $10\ kg/m^3$. The isentropic cavitation model implemented assumes that phase change from pure liquid to liquid-vapor mixture starts at $P_{vap} = 2340\ Pa$ which corresponds to the vapor pressure at temperature $293.15\ K$. The pressure decreases along the isentropic path with increasing vapor void fraction i.e. with decreasing liquid-vapor mixture density. The temperature difference between $293.15\ K$ and $292.15\ K$ corresponds to the increase in temperature along the isentropic path assuming that all the initial vapor content of the bubble would turn into liquid. The *3D* spherical bubble is initialised inside the flow domain at time $t = 0\ s$ with initial bubble radius $R_0 = 500\ \mu m$. The surrounding liquid is initialized with a $P_{\infty} = 10\ MPa$ and the bubble starts to collapse at $t > 0\ s$ under the influence of the surrounding liquid pressure. The computational domain for the *3D* simulation is cubical in shape with numerical boundaries located at $25\ R_0$ away from the bubble center in all dimensions. The bubble is spatially resolved with *100* cells in the initial bubble radius R_0. The bubble interface is defined by the variation of vapor void fraction $\alpha = 0$ in the pure liquid to $\alpha = 0.99$ inside the bubble.

The time step for the resolved problem is $\Delta t_{CFD} = 5{\cdot}10^{-10}\ s$ based on *CFL* and acoustic *CFL* condition. The total simulated collapse is completed within the computed Rayleigh time $t_{rayleigh}$ of $4.6{\cdot}10^{-6}$ s. The comparison of the simulated *3D* bubble collapse by the developed $YALES2$ compressible cavitation solver and theoretical Rayleigh-Plesset collapse is shown below in figure 2. The plot shows the evolution of bubble radius R with respect to time t, both normalized by initial bubble radius R_0 and Rayleigh time $t_{rayleigh}$ respectively. The solid line is the solution obtained from Rayleigh-Plesset analytical equation and the dotted solid line represent the equivalent radius from the total bubble vapor volume content obtained from the simulation. A decent agreement between the analytical and numerical result is obtained during the collapse, demonstrating the ability of the developed compressible cavitation solver to predict the dynamics of bubble collapse effectively.

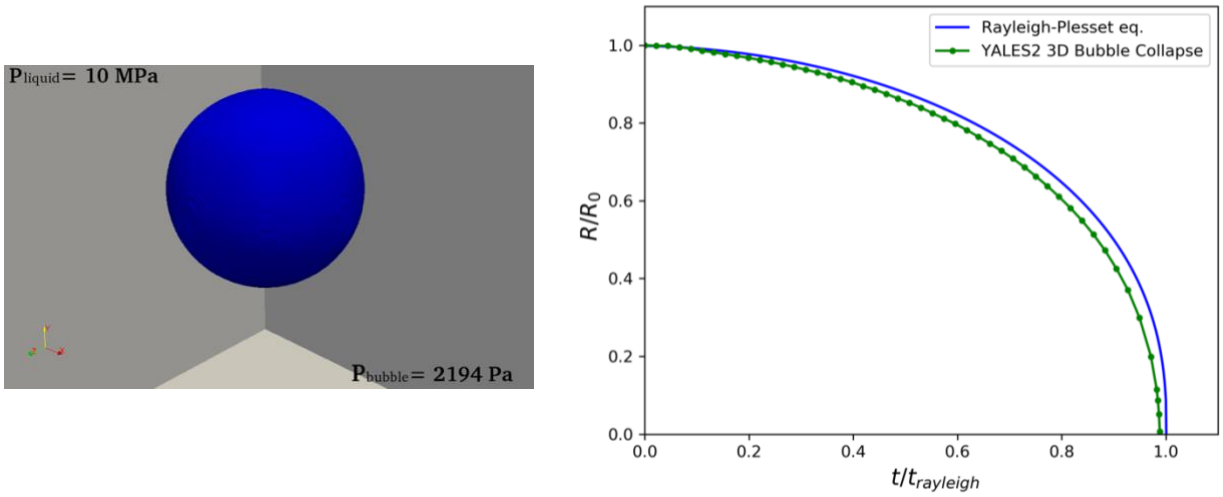

Figure 2 :Simulation of a single *3D* spherical bubble collapse with $YALES2$ and comparison with Rayleigh Plesset collapse model for $R_{max} = 500\ \mu m$, $P_{\infty} = 10\ MPa$. Numerical bubble collapse setup (left); evolution of non-dimensional radius with respect to non-dimensional time (right)

Further, the collapse of an isolated vapor bubble attached to a solid boundary is investigated in a *2D* setup. The initial radius of the bubble is $R_0 = 500\ \mu m$ and the bubble is placed near the boundary as such to obtain a stand-off parameter of 0.8. The bubble is initialised with a vapor void fraction $\alpha = 0.99$ saturated inside at vapor pressure $P_{vap} = 2194\ Pa$ and surrounded by liquid pressure of $P_{\infty} = 100\ MPa$. The bubble is placed on the bottom surface of

a rectangular domain which is numerically treated as a rigid boundary. An acoustically non-reflecting outlet boundary condition is imposed at other faraway boundaries of the rectangular domain situated $25R_0$ distance away from bubble center to avoid the interaction of reflected shock waves with the final stages of the collapse. The bubble is spatially well resolved with *100* cells along the initial bubble radius R_0. The problem was simulated with a temporal resolution of $\Delta t_{CFD} = 5.10^{-10}\ s$, chosen from the minimum time step computed from *CFL* and acoustic *CFL* condition during the moment of collapse and kept constant throughout the computation. Figure 3a shows the initial set up of the *2D* bubble geometry at $t = 0\ s$. The bubble interface remains well defined during the complex collapse phase and a liquid micro-jet is formed during the final stages of the collapse from the opposite side of the rigid boundary due to asymmetry of the problem. The pressure evolution at a point *K* on the bottom boundary surface is presented in figure 3b, extracted at every $0.1\ ns$ during the simulated collapse. The considered point *K* is located right under the bubble to capture the pressure evolution due to impacting liquid jet and subsequent shock waves. The initial pressure on the point is the saturation vapor pressure $P_{vap} = 2194\ Pa$ due to the attached bubble on the boundary. It is assumed that there is no liquid film layer between the attached bubble and solid boundary. Until $t = 3.0326\ \mu s$, the pressure at the point remains at P_{vap} as the bubble shrinks and formation of micro-jet starts. Two distinct pressure peaks can be seen in the pressure plot at $t = 3.0715\ \mu s$ and $t = 3.2079\ \mu s$ of $1986\ MPa$ and $3920\ MPa$ respectively. The first observed pressure peak is due to liquid jet impact and second peak due to the collapse of the bubble ring or torus, similar to the observations made in *Chahine et al.* [7].

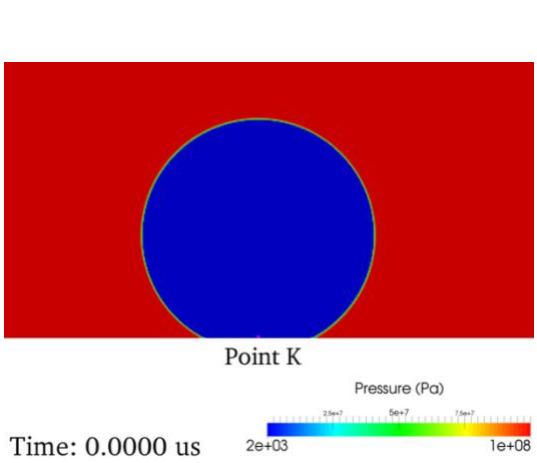

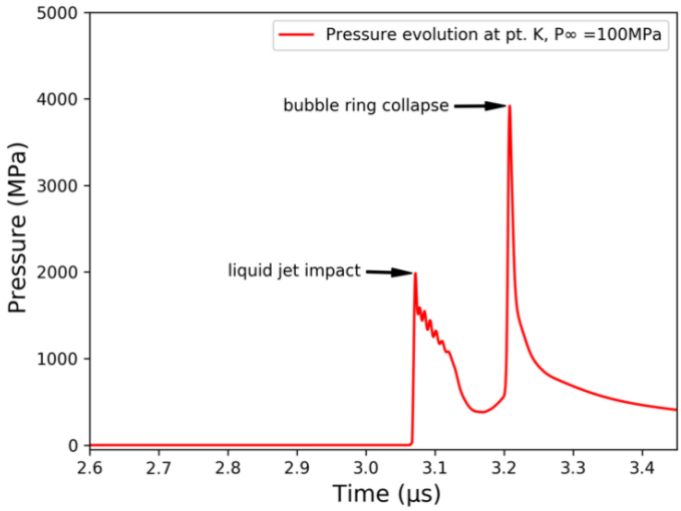

Figure 3a (left) : : Initial bubble setup with represented point *K* in the bottom solid boundary where pressure evolution is plotted; Figure 3b(right): Pressure evolution at point *K* in the bottom solid boundary, $R_{max} = 500\ \mu m$, $\gamma = 0.8$, $P_\infty = 100\ MPa$

The corresponding pressure and density contours for the observed pressure peaks are shown next in figure 4 and figure 5. The first pressure peak of $1986\ MPa$ is the liquid jet with an estimated velocity of $880\ m/s$ impacting the solid boundary and producing an instantaneous water hammer like pressure load at $t = 3.0715\ \mu s$.

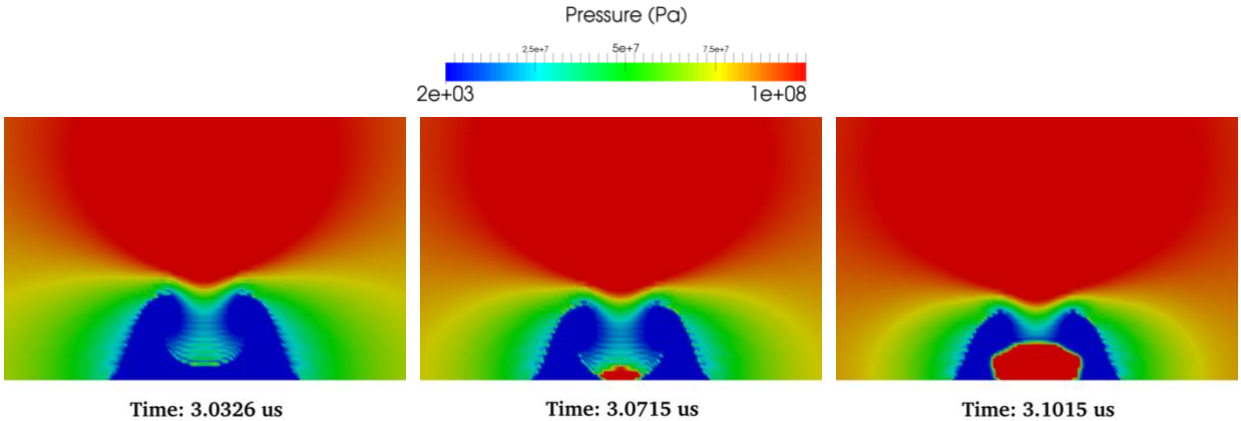

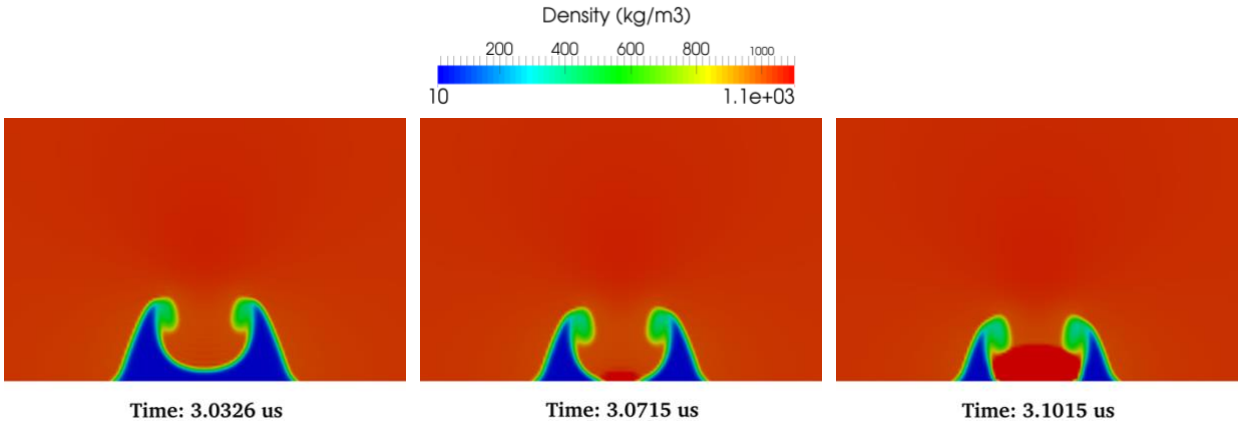

Figure 4: Pressure (top) and density (bottom) contour for a *2D* bubble collapse showing the liquid micro-jet impacting the solid boundary, corresponding to the first pressure peak of *1986 MPa* seen at time *t = 3.0715 μs*

The remaining bubble ring after the liquid micro-jet impact contracts due to the surrounding liquid pressure towards the center of the bubble. The impacting liquid jet rebounds from the solid boundary and contributes to the shrinking of remaining vapor bubble ring. The remaining bubble ring is thus, impacted by an inward moving flow surrounding the bubble and an outward moving flow from the liquid jet rebound. As the bubble ring collapses, two shock waves are emitted that travel through the domain with liquid speed of sound. The second pressure peak of $3920\ MPa$ is created at $t = 3.2079\ \mu s$ due to the interaction of the travelling shock waves at the bubble center as seen in figure 5.

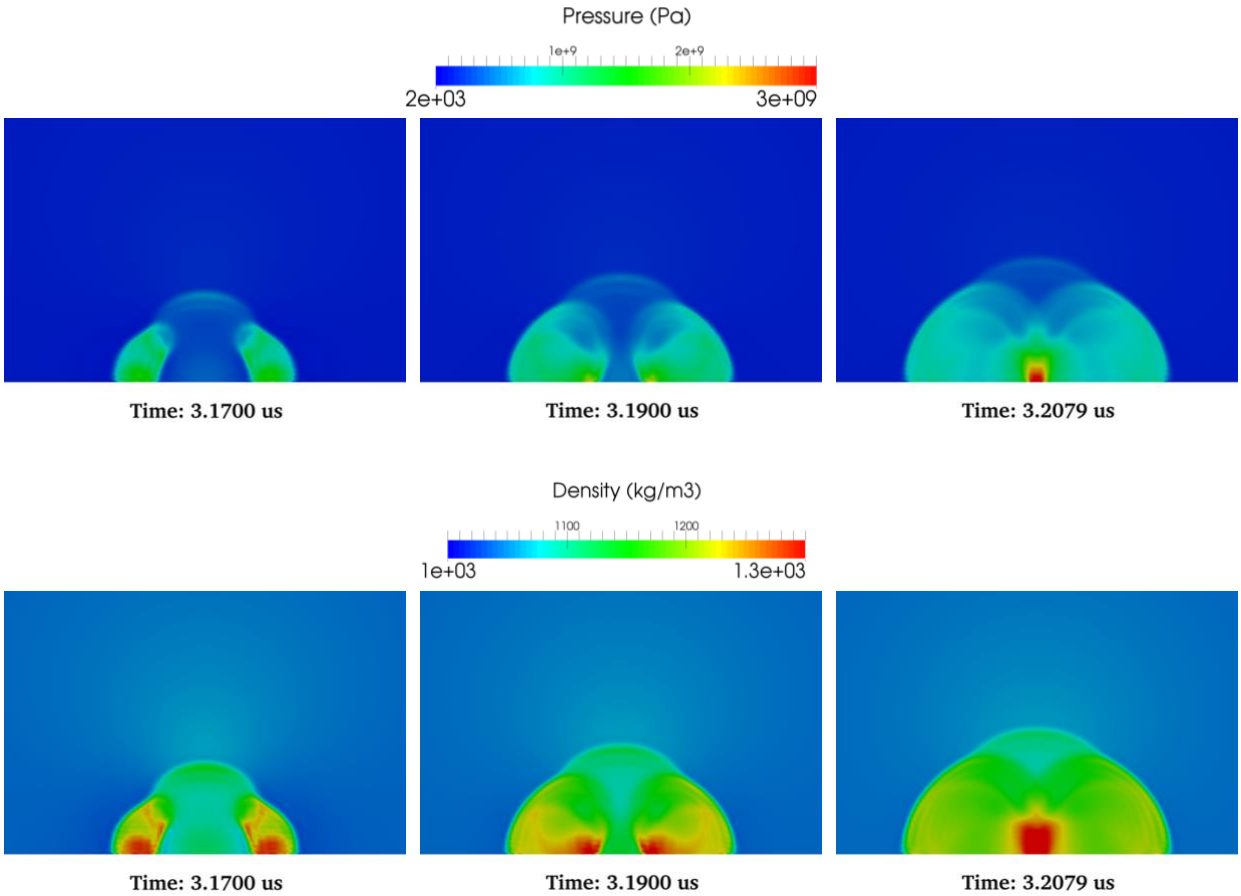

Figure 5: Pressure (top) and density (bottom) contour for a *2D* bubble collapse showing the interaction of shock waves after the collapse of the bubble torus, corresponding to the second pressure peak of *3920 MPa* at *t = 3.2079 μs*

Conclusion

This work has been devoted to the investigation of the dynamics of a single vapor bubble collapse. The fluid is assumed to be compressible and viscous for the problem. Using the described numerical method, a *3D* bubble collapse in an unbounded fluid has been realised and compared with the analytical Rayleigh-Plesset result. There is good agreement between the numerical simulation and analytical result for the *3D* bubble collapse case. The compressible cavitation solver developed is used to investigate the collapse dynamics of a vapor bubble near a solid boundary in a *2D* set up, for an initial bubble radius $R_0 = 500\mu m$ and stand-off parameter $\gamma = 0.8$. The bubble collapses under the influence of surrounding liquid pressure $P_\infty = 100\,MPa$ and two distinct pressure peaks are observed. The first peak of $1986\,MPa$ is due to impacting liquid micro-jet and a much stronger second pressure peak of $3920\,MPa$ from the interacting shock waves after the collapse of bubble ring. This predicted instantaneous pressure will be used in the *FSI* methodology to predict the solid boundary response.

References

[1] Franc, J.-P., Michel, J.-M. (2004). *Fundamentals of Cavitation*. Kluwer Academic Publishers, Dordrecht.

[2] Philipp, A., Lauterborn, W. (1998). *Cavitation erosion by single laser-produced bubbles*. J. Fluid Mech., vol. 361.

[3] Moureau, V., Berat, C., Pitsch, H. (2007). *An efficient semi-implicit compressible solver for large-eddy simulations*. J. Comput. Phys. 226.

[4] Kim, J., Moin, P. (1992). *Application of a fractional step method to incompressible Navier Stokes equations*. J. Comput. Phys. 101.

[5] Poinsot, T., Lele, S. (1992). *Boundary Conditions for Direct Simulations of Compressible Viscous Flows*. J. Comput. Phys. 101.

[6] Egerer, C. et al. (2013). *LES of turbulent cavitating shear layers*. in Nagel, W.E. et al. (eds.), High Performance Computing in Science and Engineering, Springer.

[7] Chahine, G.L., Hsiao, C.-T. (2015) *Modelling cavitation erosion using fluid-material interaction simulations*. Interface Focus 5: 20150016.